Sveriges lantbruksuniversitet
Swedish University of Agricultural Sciences

Department of Soil and Environment

Quantifying relationships between X-ray imaged macropore structure and hydraulic conductivity

Muhammad Arslan Ahmad

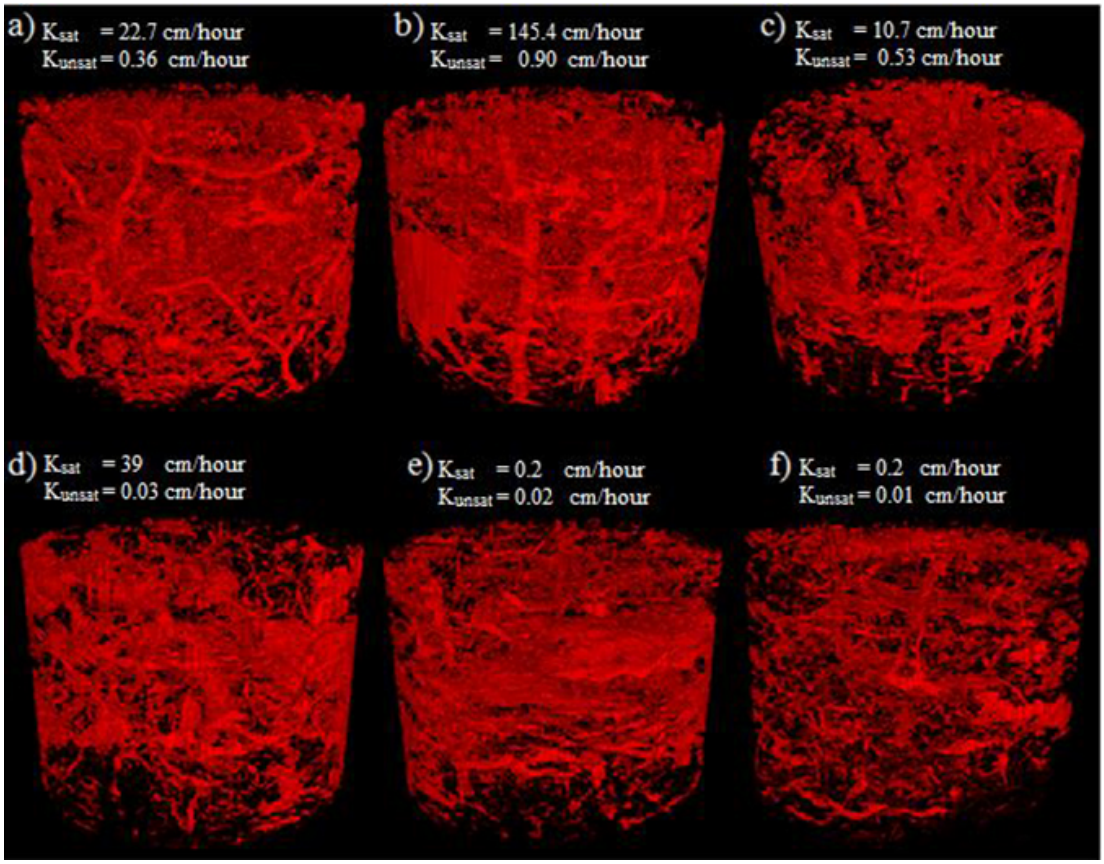

Master's Thesis in Environmental Science
Soil and Water Management – Master's Programme

Examensarbeten, Institutionen för mark och miljö, SLU
2016:11

Uppsala 2016

Quantifying relationships between X-ray imaged macropore structure and hydraulic conductivity

Muhammad Arslan Ahmad

Supervisor: Nicholas Jarvis, Department of Soil and Environment, SLU
Assistant supervisor: Johannes Koestel, Department of Soil and Environment, SLU
Examiner: Ingmar Messing, Department of Soil and Environment, SLU

Credits: 30 ECTS
Level: Second cycle, A2E
Course title: Independent Project in Environmental Science - Master´s thesis
Course code: EX0431
Programme/Education: Soil and Water Management – Master's Programme 120 credits

Place of publication: Uppsala
Year of publication: 2016
Cover picture: 3D-visualization of pore space in soil columns together with measured hydraulic conductivity, 2016, photo by author
Title of series: Examensarbeten, Institutionen för mark och miljö, SLU
Number of part of series: 2016:11
Online publication: http://stud.epsilon.slu.se

Keywords: critical pore diameter, modelling, pedotransfer functions, physics based approaches, SoilJ, 3-D visualization, soil characterization

Sveriges lantbruksuniversitet
Swedish University of Agricultural Sciences

Faculty of Natural Resources and Agricultural Sciences
Department of Soil and Environment

Abstract

Computer based simulation models which estimate hydraulic properties of soil usually make use of statistical approaches such as multiple regressions that relate hydraulic properties to widely measured soil properties like textural fractions, organic matter content and bulk density. The problem is that hydraulic properties are usually only weakly correlated to these properties, because it is more strongly dependent on the characteristics of larger pores in the soil. The characteristics of macropore in soil can be determined by X-ray tomography. The aim of this study was to evaluate the predictive performance of X-ray CT derived macropore characteristics for hydraulic properties of soil.

Twenty undisturbed soil cores were sampled (6 cm high, 6.5 cm diameter) from a soil pit, with replicate cores taken at different depths from clay soil in Skuterud catchment, Norway. Hydraulic properties', including saturated hydraulic conductivity, was measured using constant head method and unsaturated hydraulic conductivity was measured using Mini-Disk Infiltrometer. Soil columns were scanned using X-ray CT scan at a voxel resolution of 40 microns. Minimum automatic threshold algorithm method was chosen to segment the images between pore space and soil matrix. The images were analyzed for quantifying the macropore characteristics using ImageJ, SoilJ, BoneJ and GeoDict.

Significant correlations were observed between hydraulic conductivity and most CT derived macropore characteristics. Many of the X-ray CT derived macropore characteristics were interrelated. Best multiple linear equations for predicting the saturated and unsaturated hydraulic conductivity were estimated from macropore characteristics. Among the macropore characteristics critical pore diameter largely contributed to the saturated hydraulic conductivity. Macroporosity and connected macroporosity mainly controlled the unsaturated hydraulic conductivity. Physics-based approaches like percolation models based on critical pore diameter serves better than statistical approaches for decision making in soil and water management.

Popular Science Summary

Hydraulic conductivity is the measure of ease by which the soil pores permit the flow of water in soil. If the flow of water occur under saturated conditions of the soil it is called saturated hydraulic conductivity, otherwise it is called unsaturated hydraulic conductivity. Flow of water in soil determines the plant water uptake and transportation of solute in soil. The rate of flow of water in soil regulates that either water will infiltrate in soil or evaporate from the soil. Knowledge of hydraulic conductivity is useful for hydrologic models like watershed modelling, storm water management and land use planning for both urban and agriculture life. Computer based simulation models are used to predict the flow of water in soil.

These models require data regarding hydraulic properties of soil such as hydraulic conductivity and unsaturated hydraulic conductivity for predicting the flow of water in soil. These models generally relate the flow of water with basic soil properties such as texture and organic matter etc. But in reality the fast flow of water is mainly controlled by the larger pores (macropores) in soil. Advancement in X-ray computed tomography has made it possible to quantify the characteristics of macropores. X-ray computed tomography gives us more reliable, detailed and accurate results which increase our understanding about the soil process. In this study we quantify the characteristics of larger pores in soils to predict the flow of water in soil. Our objective was to statistically analyze the relationship between saturated and unsaturated hydraulic conductivity with X-ray derived macropore characteristics.

Soil columns (6 cm high, 6.5 cm diameter) were scanned at image resolution of 40 microns. Macropore characteristics such as total large pore spaces (macroporosity), connected large pore spaces from top to bottom (connected macroporosity) and the smallest diameter at fastest flow path (critical pore diameter), mean thickness of the lager pore cluster and anisotropy etc. were measured using X-ray computed tomography. Saturated hydraulic conductivity was measured using constant head method and a mini-disk infiltrometer was used to measure the unsaturated hydraulic conductivity.

Soil columns were visualized in 3 dimensions. It was observed that larger hydraulic conductivities values are associated with larger, less tortuous macropores which are connected from top to bottom. Smaller hydraulic conductivity values were associated with smaller macroporosities and lack of macropore clusters which are connected from top to bottom. An earthworm was detected in one of the soil column and multiple macropore connection in horizontal and vertical direction presumably associated with the movement of the earthworm.

Strong correlations were observed between macropore characteristics and hydraulic properties of soil. It was concluded that saturated hydraulic conductivity is mainly predicted by the critical pore diameter and unsaturated hydraulic conductivity is mainly predicted by macroporosity and pore spaces which were connected from top to bottom. Strong interrelation between macropore characteristics limits their use for predicting the hydraulic conductivity using statistical approaches. Therefore models founded on the principal of physics like percolation models based on critical pore diameter can be the best alternative. This research gave a vision for future soil characterization and future fluid simulation models may use segmented X-ray CT derived data for predicting the hydraulic conductivity.

Contents

List of tables

List of figures

Abbreviations

Aniso	Anisotropy index
ca.	Approximately
CT	Computed tomography
D_{crit}	Critical pore diameter
DDA	Digital detector array
DXR	Digital X-ray radiogrammetry
etc.	Et cetera
Eular no.	Euler number
FAO	Food and Agriculture Organization
FracD	Fractal dimension
GE	General electric
K	Hydraulic conductivity
K_{sat}	Saturated hydraulic conductivity
K_{unsat}	Unsaturated hydraulic conductivity
MeanT	Mean thickness
MP	Macroporosity
MPC	Connected macroporosity
ROI	Region of interset
RT	Real time
S^2	Variance
SCO	Scan optimizer
SE	Standard error
TIFF	Tagged image file format

1. Introduction

Computer based simulation models are used in decision-making in soil and water management, especially to solve problems related to land use and environment. Quantified soil data is required including hydraulic parameters such as saturated hydraulic conductivity to estimate the parameters of the computer based simulation models. Since field measurements are time consuming and labor demanding, we can measure these hydraulic parameters at some locations, but not everywhere, so we need methods to estimate them.

Saturated hydraulic conductivity is important physical parameter for defining the transport of solute and water in soil. Knowledge of saturated hydraulic conductivity is useful in hydrologic models including watershed modelling, storm water management, land use planning and designing septic systems (Arrington *et al.*, 2013). Saturated hydraulic conductivity is rarely included in routine soil survey as it is expensive to measure, consume a lot of time and have high degree of spatial variability. As results saturated hydraulic conductivity is being estimated by the pedotransfer functions (Minasny & McBratney, 2000).

Empirical models have been developed which use statistical approaches such as multiple regression to relate saturated hydraulic conductivity to widely measured soil properties like texture fractions, bulk density and organic matter content (Jabro, 1992) (Rawls *et al.*, 1998). The problem is that saturated hydraulic conductivity is usually only weakly correlated to these properties (Vereecken *et al.*, 2010), because it is more strongly dependent on the characteristics of larger pores in the soil, termed macropores.

Macropores in soils are formed from the borrowing of earthworm, decomposing of plant roots, swelling-shrinkage of soils (cracks), and agriculture management practices like ploughing (Jarvis, 2007). Macropores (cylindrical diameter > 0.3-0.5mm) normally constitute a small fraction of the soil but still contribute to the major flow of water in soil at saturation (Jarvis, 2007).

Some pedotransfer functions which account for the soil structure for predicting the saturated and near saturated hydraulic conductivity have been developed. For example, soil structure is a key parameter for predicting the hydraulic properties of the soil in macropore flow region (Lin et al., 1999) and saturated hydraulic conductivity can be reasonably predicted from the effective porosity in clay soils (Messing, *1989*). Minasny & McBratney. (2000) developed some pedotransfer function for predicting hydraulic conductivity by using fractal dimension and effective porosity. Iversen *et al.* (2012) found a strong correlation between saturated hydraulic conductivity and macropore density.

X-ray CT scanning can be used to quantify macropore characteristics non-destructively in three dimensions. X-ray CT technology gives more reliable, detailed and accurate information which increase our understanding about the soil process (Viggiani et *al*., 2015). Over the last decades various studies on the characterization of macropore structure were conducted (Pierret *et al.*, 2002; Udawatta *et al.*, 2008; San José Martínez *et al.*, 2010; Wildenschild & Sheppard, 2013; Paradelo *et al.*, 2016) and X-ray CT is considered as reliable and accepted technique for studying and characterizing the complex process of the soil. Larsbo *et al.* (2014) and Paradelo *et al.* (2016) have observed a good correlation between X-ray imaged macropore characteristics and flow of water in soil.

The objective of this thesis is to statistically relate the X-ray CT derived macropore network characteristics with the hydraulic conductivity and to evaluate which characteristics that best predict the hydraulic conductivity. Our results might increase our confidence in one of these characteristics

used for predicting the hydraulic conductivity. The work is done as the part of the project "Quantifying Soil Structure to Augment the Relevance of Laboratory-Based Soil Hydraulic Properties for Environmental Modelling" (SoilSpace).

2. Review of literature

2.1. Hydraulic properties

Hydraulic conductivity, K, is the measure of the ease by which soil pores permit the flow of water. If the water is flowing under saturated soil conditions then it is called saturated hydraulic conductivity (K_{sat}) otherwise it is called unsaturated or near saturated hydraulic conductivity (K_{unsat}). The flow of water in soil is important for both urban and agriculture life. The rate of flow of water in soil plays an important role determining whether water evaporates or infiltrates, its movement to plant roots, drains and wells (Black *et al.*, 2006).

Saturated and unsaturated hydraulic conductivity can be measured in both the laboratory (Klute *et al.*, 1986a) and in the field (Klute *et al.*, 1986b). Measuring the hydraulic properties of soil is, however, difficult, expensive and time consuming which is why it is not usually included in routine soil surveys. The widespread need for knowledge of hydraulic conductivity (K) in solving agricultural and environmental problems means that indirect methods are needed to estimate K (Bouma, 1989).

2.2. Pedotransfer functions

Pedotransfer functions provide the means of estimating K_{sat} values from basic soil properties. The estimated hydraulic properties then can be used in solving problems related to agricultural management and the environment. For example, Smettem *et al.* (1999) used hydraulic properties predicted by pedotransfer functions in spatial modelling of water storage to estimate the yield of wheat crops. Soil texture was the first parameter to be used in estimating K_{sat} as it provides information about poorly drained or freely drained pore spaces available for water flow. Soil texture is easy to measure and readily available from soil surveys for particular areas of interest. Rawls *et al.* (1998) added bulk density as a predictor variable in the pedotransfer functions as it also provides information regarding soil porosity. Soils of the same texture class but greater porosity (smaller bulk density) will have larger hydraulic conductivity. The assumption with these relationships is that soils with similar soil texture will develop similar pore architecture, but in reality this may not hold true as soil structure and pore architecture may differ, depending, for example, on climate and frequency of soil drought. Wagner *et al.*, (1998) reported poor relationships between soil texture and the hydraulic properties of soil. Arrington *et al.*, (2013) found that including non-soil parameters such as elevation, slope, aspect with basic soil properties to predict the hydraulic properties of soil did not improve the accuracy of the estimation. Jarvis *et al.* (2013) found that besides soil texture and bulk density, organic carbon, land use and soil management practices were important factors determining K in soil .

Soil structure strongly influences the hydraulic properties of soil. The presence of macropores in soil complicates the estimation of hydraulic properties. Messing *(1989*) found significant relationship between spatial distribution of saturated hydraulic conductivity and effective porosity determined from soil water retention characteristics in clay soils. Organic matter has been used in predicting the hydraulic properties of soil as it affects soil structure (Nemes *et al.*, 2005). Furthermore, soil morphological features and pedological descriptions from soil survey have also been included as soil structure parameters to predict the hydraulic properties of soil. For example, Lin et al. (1999) found that the abundance and size of the macropores were crucial parameters for estimating saturated hydraulic conductivity.

2.3. X-ray CT scanning

X-ray tomography provides a convenient way of quantifying at high resolution the 3D geometry and connectivity of the macropore structures which contribute to the hydraulic properties of soil (Pierret *et al.*, 2002; Viggiani et *al*., 2015). Several studies have used X-ray measurements of the characteristics of macropores to predict the flow of water in soil. Luo *et al.*, (2010) found that macropore characteristics such as macroporosity, hydraulic radius and path number were correlated with saturated hydraulic conductivity. Iversen *et al.* (2012) found that the flow of water in macropores is significantly related with macropore density at saturated condition of the soil. Larsbo *et al.* (2014) found significant correlations of macropore characteristics measured by X-ray (macroporosity, macropore surface area, aggregate thickness and connectivity) with near-saturated hydraulic conductivity of soil. The study also confirms the interrelation of many macropore characteristics. Most recently, Paradelo *et al.* (2016) reported that X-ray CT derived macropore characteristics such as macroporosity and limiting macroporosity (soil macroporosity along the vertical axis) had significant correlations with saturated hydraulic conductivity. The soil layers with smallest macroporosity control the macropore flow and restrict the flow of water from the whole soil column.

3. Materials and Methods

3.1. Site details, soil sampling and preparation

The soil was sampled from the Skuterud catchment which is located in the Ås municipality, approximately 30 km south of Oslo in southern Norway. The total area of the Skuterud catchment is 4.5 km^2 and the altitude above sea level varies from 85 to 150 m. The mean annual precipitation of the catchment is 785 mm with the mean annual temperature of 5.3° C (Starkloff & Stolte, 2014). The soils of the sampling area can be classified as Stagnosols (FAO soil classification system) which were formed from marine sediments and have large amounts of silt and clay (Haraldsen, 2015, pers. comm., 23 October). The major land use in the Skuterud catchment is cereal production, which covers approximately 60 % of the total catchment area. The land use in the remaining area consists of a pine plantation (33%) and built-up areas (7%) (Kværnø *et al.*, 2007).
Twenty undisturbed soil cores were sampled in aluminum pipes (6 cm high, 6.5 cm diameter) on September 9, 2015 after wheat harvest from a soil pit, with replicate cores taken at different depths (Table 1). A hammer was used to push the aluminum cores (with sharp bottom cutting edge) vertically into the soil. Samples were weighed in Norway and transported to Sweden as it was planned to X-ray them in Uppsala.

Table 1 *Frequency of sampling at each depth and their corresponding weights (grams).*

Depth	Soil type	Number of samples	Average weight at each depth (grams) soil+ aluminum ring		
			After soil sampling	At -100 cm matric potential	At saturating state
05-10 cm	Clay	5	508.64	506.76	523.76
20-25 cm	Clay	3	486.84	485.05	533.59
30-35 cm	Clay	6	510.30	508.94	531.77
50-55 cm	Clay	2	544.52	543.79	559.62
70-75 cm	Clay	4	549.78	548.93	565.10

On arrival in Uppsala on January 12th, 2016, the soil inside the cores was secured by placing two plastic caps at each end and wrapping the cores with two rubber bands. The samples were placed on a sand bed after removing the caps, to equilibrate for approximately two weeks at a matric potential of -100 cm. The samples were kept on the sand bed until there was no change in weight. This was done to ensure that pores larger than about 30 microns would be air-filled. This makes it easier to distinguish the pore space during segmentation of the X-ray images. Any dirt around the soil sample was removed to ease the process of finding the column outline and for better contrast between soil and column.

3.2. X-ray Scanning

X-ray CT scan has three common parts: X-ray source, sample holder and a detector. X-rays are directed on the sample at multiple angles, sample becomes a source of electron and X-rays due to atomic interaction. Some of the primary X-rays from the source get absorbed or scattered from the sample. The change in primary X-ray intensity reaching at detector is called attenuated X-rays. This attenuation of X-rays is described by Beer's law and by the use of special algorithm like Feldkamp algorithm (Feldkamp *et al.*, 1984) the distribution of X-ray attenuation is reconstructed as scanned image.

3.2.1. X-ray machine

The X-ray scanner (GE phoenix v| tome| x m) at the Swedish University of Agricultural Sciences in Uppsala was used for scanning the soil samples. The CT system is a cone-beam micro-focus (spot size normally placed in the range of 1-10µm) installed with DXR250 Real-time (RT) digital detector array (DDA). DXR250RT detector enables consistent imaging with less calibration under temperature controlled environment.

3.2.2. Parameters for scanning

The soil core was placed in the sample holder in the scanner. A thick copper sheet of 0.7 mm was used as filter and placed in front of the detector screen to minimize beam hardening effects. The manipulator was moved on the z-axis to +0163.517 mm and on y-axis to +0372.834 mm for obtaining a voxel resolution of 40 microns. The density of the sample and its diameter determine the voltage, current, timing and sensitivity of the detector crystals used for sending the X-ray from the sample. X-ray power can be defined as the product of voltage and current as shown in equation 1.

$$Power(p) = Voltage\ (V) * Current\ (I) \qquad (1)$$

Voltage has a direct relationship with the speed of electrons and higher voltage means that electrons will pass through without interaction with sample. Current is directly related with the number of electrons and higher current means more photons will be generated to interact with the sample which reduces the time of exposure for scanning.
Lower X-ray power results in an improved contrast of the X-ray image. But if a too low power setting is chosen, there are not enough X-ray photons passing through the densest parts of the imaged object to the DXR250 sensor array. This will lead to underexposed X-ray images. The power of the X-ray scan was adjusted to 42 watt by adjusting the voltage to 150KV and current 280µA.
The crystals in the detector normally shows an after-glow which require sometime to decline. It's important to not consider at least one image after the manipulator has moved to the new position. During scanning, four radiographs were acquired from the same angle and then three of them were averaged. The total number of the scanned radiograph was 2000. The detector sensitivity was

adjusted to 2 and the total scanned area was set to 2014 by 2014 pixels. Sensor calibration was done to minimize the ring artifacts and the Auto SCO (scan optimizer) function was activated to remove the artifacts relating movement of the sample (deformation) during scanning. The sensor shift function was also activated to remove the ring artifacts.

3.2.3. Image reconstruction

Image reconstruction was done with the Phoenix datos |x CT software. The software combines the 2000 radiographs from different angles using the Feldkamp algorithm (Feldkamp *et al.*, 1984) to create a 3-D image. The output type of the reconstructed 3-D image was set to 16 bit. Beam hardening correction (bhc+) and Scan optimizer functions were applied for removing the drift effect. After reconstructing, the 3-D image was exported as a tagged image file format (TIFF-file) and saved for image processing.

3.3. Image processing

3.3.1. Scaling

Image processing was mainly done in ImageJ (Abràmoff *et al.*, 2004) by using SoilJ plugin (Koestel, 2016). The images were scaled to a resolution of 80 µm, since the larger pores (Pores diameter > 0.16 mm) were the main interest in this study. This also decreases the processing time for the scanned images. Bilinear interpolation was applied on the entire stack of the image during scaling.

3.3.2. Straighten and Centering

This algorithm in SoilJ reads the image and searches for the location and orientation of the image and places the image straight and moves it to the center of the canvas.

3.3.3. Column outline

Next the columns' inner and outer perimeter as well as the top and bottom of the aluminum columns were automatically determined using the 'column outline' function of SoilJ. This information was used in specifying the region of interest (ROI) for image analyzing. The results of the 'column outline' function were confirmed by using the debug mode of the same function.

3.3.4. Normalization

The gray values of the images were normalized for the illumination correction in the vertical direction. Normalization algorithm went through each slice of the image and scaled the gray values of the image with respect to standard values for air-phase and the aluminum wall of the column. The gray values of the air change outside the column due to artifact so the reference value of the air was selected from inside the column. Air is associated with less gray value being less dense material in image. Gray values of the air and column were detected around 5000 and 20000 in each column so the reference grey values of the air and wall of the column were adjusted to 5000 and 20000 respectively.

3.3.5. *Histogrammer*

A joint histogram of all the images, as shown in Fig. 1, was obtained by running the histogrammer algorithm on all the scanned soil images.

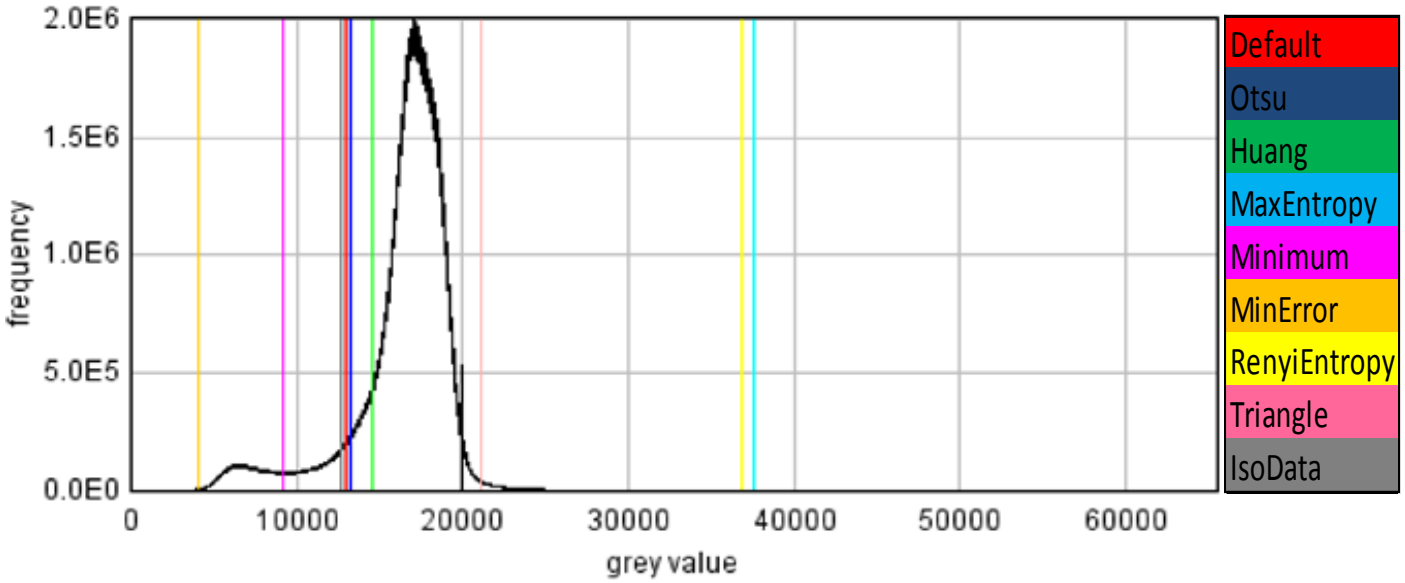

Figure 1 *A joint histogram of all soil images with colored line showing several automatic thresholding algorithms. Scale bar showing the color codes for each threshold algorithm*.

3.3.6. *Segmentation*

By looking at the joint histogram of the images as shown in fig 1, a clear minimum peak between air and matrix density at 9216 gray value, minimum automatic threshold method (Prewitt & Mendelsohn, 1966) was chosen to segment the image between pore space and soil matrix. This threshold level was applied on all the images and it gave good results as compared to the other methods. It was observed that a slight increase in the threshold value resulted in segmenting organic matter as pore space.

3.3.7. *Soil Surface Finder*

Function of soil surface finder was applied which look from top to bottom and make a topographic map from the top surface and bottom surface. It was done to specify identical soil volume in each column.

3.3.8. *Quantification of macroporosity*

Macropore morphologies in the binary images were quantified using the "pore space analyzer" available in SoilJ, which for the last part relies on the BoneJ plugin (Doube *et al.*, 2010). Pore space analyzer provides the opportunity to look at whole image or to look at the each macropore cluster individually. Mean thickness of the macropore network were calculated by using BoneJ, a plugin in ImageJ. The "zero" values of connected macroporosity was replaced with the minimum recorded value. The binary tiff stack image was saved as an image sequence to process in GeoDict (http://www.geodict.com) for determining the critical pore diameter. The zero value of critical pore diameter was replaced by the image resolution (80 microns). A brief description of the macropore characteristics measured on each sample is given in Table 2.

Table 2 *Measured characteristics of the macropore network.*

Characteristics of macropore	Description
Macroporosity (cm^3cm^{-3})	The total volume of macropores divided by the total volume of soil sample.
Connected macroporosity (cm^3cm^{-3})	The total volume of the pore space that is connected from top to bottom of the sample divided by the total volume of the soil sample.
Critical pore diameter (µm)	The smallest "bottleneck" diameter at the fastest flow path connected from top to bottom.
Mean thickness (mm)	Mean thickness of the pore space (i.e. mean pore size)
Fractal dimension	A measure characterizing the mass fractal pattern of macropore network.
Euler number	A measure used for local macropore connectivity.
Anisotropy index	A measure of anisotropy varying from zero (random) to 1. Higher values mean that the pore space is not randomly oriented, but has a preferred direction.

3.4. Hydraulic properties

3.4.1. Saturated hydraulic conductivity (K_{sat})

After completion of X-ray scanning, the soil samples were saturated from the bottom with a stepwise addition of 5 mm of water per day for two weeks. Water used for saturating the soil samples was boiled and kept in a closed container for overnight to remove the dissolved air from the water. The degassed water was gently poured into the sample container to avoid the air mixing in water. Saturated hydraulic conductivity was then measured using the constant head method (as shown in figure 2) in a temperature controlled laboratory.

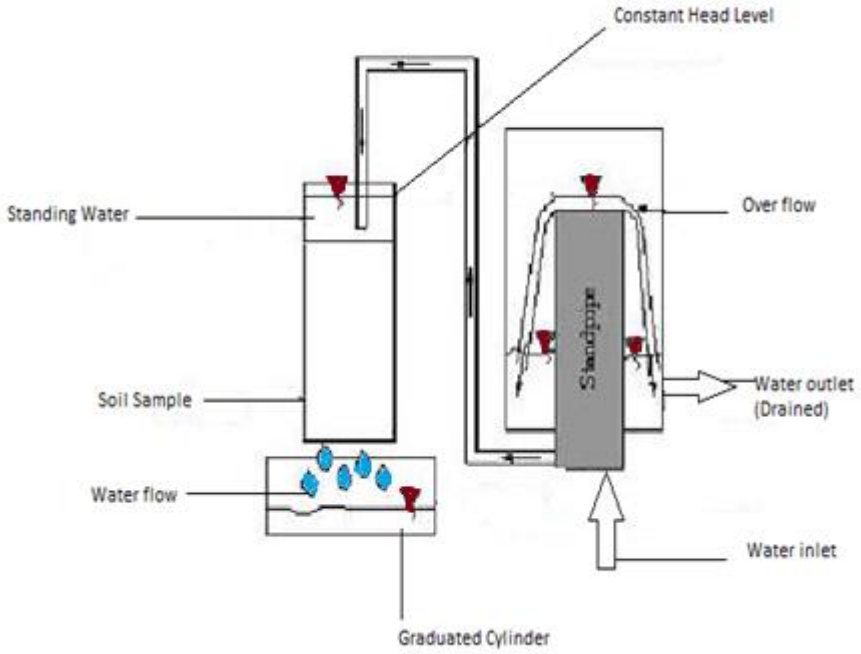

Figure 2 *Saturated hydraulic conductivity (K_{sat}) measuring device by using Constant head method adapted from the laboratory manual (Soil Properties Laboratory - Ksat Lab procedures.pdf)*

Three readings of the flow rate Q (cm^3 $hour^{-1}$) through the sample under a known hydraulic gradient were taken for each sample. The mean value of Q was then used to calculate saturated hydraulic conductivity, K_{sat} (cm $hour^{-1}$) from Darcy's Law as

$$K_{sat} = \frac{Q}{A}\left(\frac{\Delta L}{\Delta H}\right) \qquad (2)$$

where A (cm^2) is the area of the sample, ΔH (m) is the change in total hydraulic head and Δ L (m) is the change in length of the soil sample. The "zero" recorded value of saturated hydraulic conductivity was replaced with the minimum recorded value.

3.4.2. Unsaturated Hydraulic conductivity (K_{unsat})

Prior to determining unsaturated hydraulic conductivity, the soil samples were first drained on a sand bed at -100 cm matric potential for a few days. A mini-disk tension infiltrometer was used to infiltrate water into the soil using a supply matric potential of -6 cm (see fig. 3). According to the capillary rise equation, supplying water to soil at this matric potential will exclude water flow through pores larger than ca. 0.5 mm diameter during infiltration.

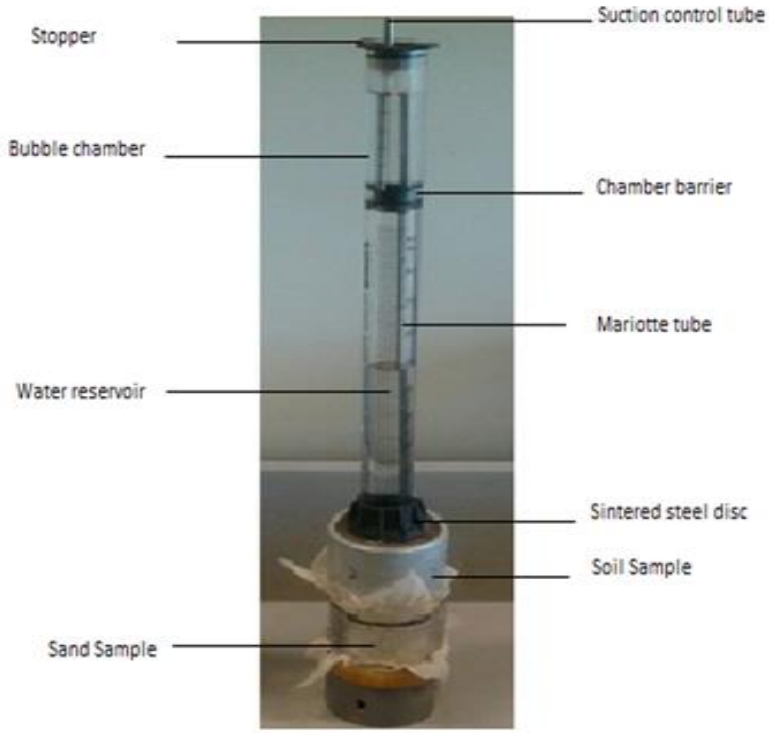

Figure 3 *Mini-Disk tension Infiltrometer used for measuring unsaturated hydraulic conductivity*.

A small amount of fine sand was added on the top surface of the soil sample to enhance the contact of the porous stainless steel disk with the soil sample during infiltration. The volume of the water in water reservoir tube was noted at time zero and the change in the water volume was recorded at regular intervals in order to calculate infiltration rate. The measurements continued until steady-state was reached. The diameter of the infiltrometer is 3.1 cm which is only slightly smaller than the core

diameter. One-dimensional vertical flow could therefore be assumed, so that the measured steady infiltration rate is equivalent to the unsaturated hydraulic conductivity at a matric potential of -6 cm.

4. Results and discussion

4.1. 3-D visualization of pore space

Fig 3. shows example images of soil columns from different depths generated by X-ray tomography with their respective measured hydraulic conductivities. The red color in soil columns represents macropores of thicknesses greater than 0.16 mm. Visual inspection of the soil columns shows that the macropores are well connected in both horizontal and vertical directions. Decreasing macroporosities with depth are often reported (e.g. Naveed *et al.*, 2013) but we did not observe any clear trends with depth for macropore characteristics and hydraulic conductivity. Looking at the soil columns shown in Fig 3. we may infer that larger hydraulic conductivities associated with Column 6, shown in **(3b)**, is due to the one large, less tortuous, macropore which is connected from top to bottom. Smaller hydraulic conductivities in column 19, shown in **(3e)**, and column 20, shown in **(3f)**, are due to the smaller macroporosities and lack of macropore clusters that connect from top to bottom. An earthworm was detected in column 1, shown in **(3a),** with multiple macropore connections in horizontal and vertical directions, presumably associated with the movement of this earthworm.

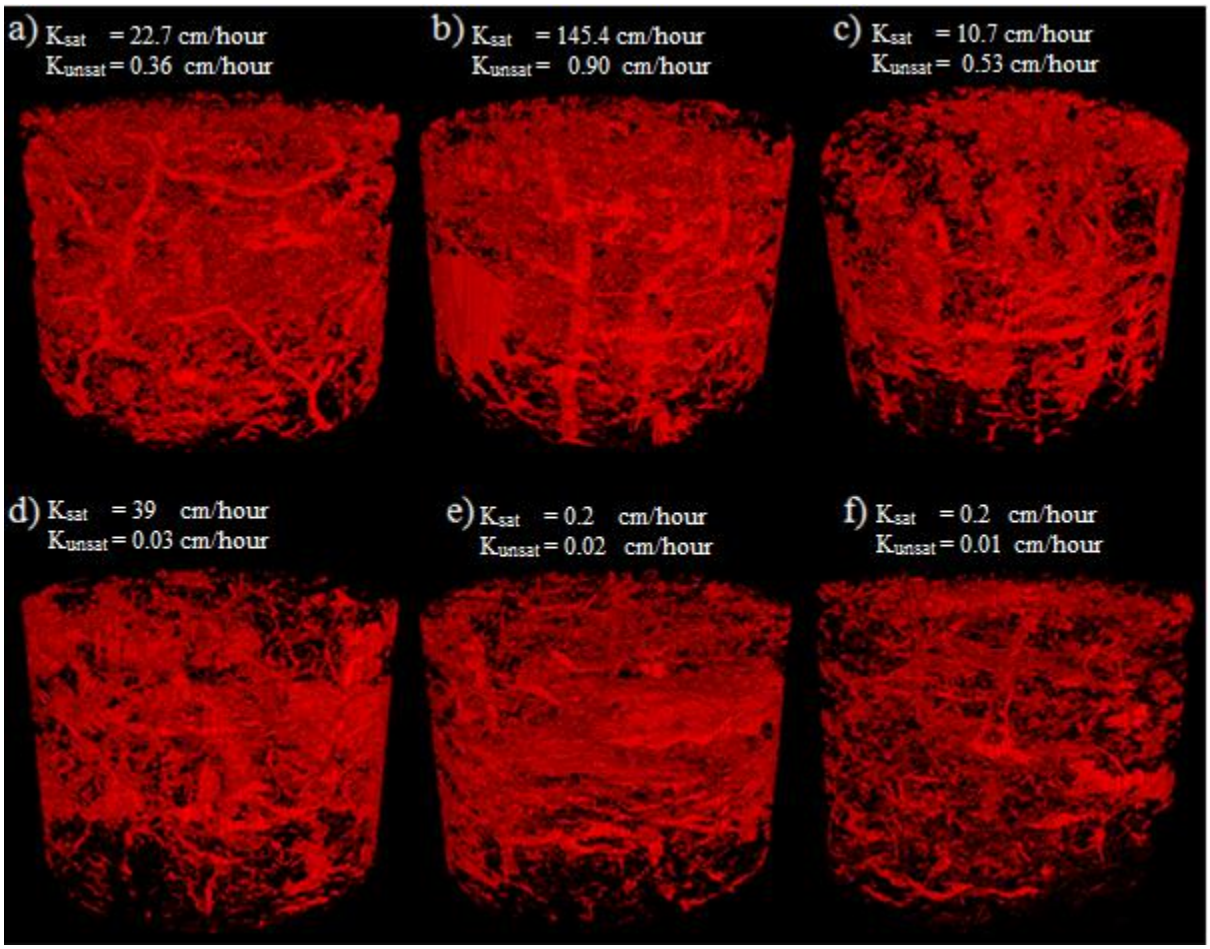

Figure 4 *Example 3-D visualizations of pore space in soil columns sampled at different depths, together with measured saturated (K_{sat}) and unsaturated hydraulic conductivity (K_{unsat}). (a) column 1 (depth 5-10 cm) (b) column 6 (depth 20-25 cm) (c) column 9 (depth 30-35 cm) (d) column 15 (depth 50-55 cm) (e) column 19 (depth 70-75 cm) (f) column 20 (depth 70-75 cm).*

4.2. Descriptive Statistics

Table 3 shows descriptive statistics for X-ray CT scanned macropore characteristics and hydraulic properties.

Table 3 *Descriptive Statistics of CT measured macropore characteristics and hydraulic properties of soil.*[1]

Variables	Mean	Minimum	Median	Maximum	Kurtosis	Skewness	Range	S2	SE
Ksat (cm/h)	20.35	0.2	6.19	145.35	10.74	2.99	145.15	1116.45	7.47
Kunsat (cm/h)	0.3	0.015	0.04	1.42	1.71	1.57	1.41	0.18	0.09
MP (cm^3cm^{-3})	0.04	0.01	0.03	0.08	0.68	1.15	0.07	0.0003	0.004
MPC (cm^3cm^{-3})	0.02	0.001	0.01	0.07	0.51	1.16	0.07	0.0005	0.005
D_{crit} (µm)	351.75	80	357.77	800	-1.09	0.32	720	54684.27	52.28
Aniso	0.23	0.09	0.2	0.58	2.85	1.47	0.49	0.01	0.02
FracD	2.35	2.17	2.32	2.58	-0.1	0.43	0.41	0.01	0.02
MeanT (mm)	60.48	33.39	54.05	127.71	2.15	1.53	94.31	691.27	5.87
Euler no.	20955.6	1875	19486	35088	-0.92	-0.26	33213	1.0E+08	2241.78

The large differences in mean and median values of the hydraulic conductivities of soil indicate that the data was not normally distributed, with some extreme values. Therefore hydraulic conductivities of the soil was log transformed in order to have normal distribution before applying statistics.

4.3. Correlations among variables

Pearson correlation coefficients (*r*) were calculated to assess the relationships between CT derived macropore characteristics and log of hydraulic conductivity. These are shown in Table 4. Significant correlations were observed between log of hydraulic conductivities and most CT- derived macropore characteristics. Very strong pearson correlations were observed for log of saturated hydraulic conductivity with critical pore diameter, mean thickness, macroporosity and connected macroporosity. In the case of log of unsaturated hydraulic conductivity, very strong correlations were found for macroporosity, connected macroporosity and fractal dimension. Many of the X-ray CT derived macropore characteristics were interrelated, which agrees with the findings of Larsbo *et al.* (2014). Connected macroporosity was strongly correlated with macroporosity. Larger macroporosities are associated with more homogeneous macropore distribution, which are well connected from top to bottom and have high surface area.

[1] X-ray CT scanned macropore characteristics includes macroporosity (MP), connected macroporosity (MPC), critical pore diameter (D_{crit}), anisotropy index (Aniso), fractal dimension (FracD), mean thickness of the largest pore cluster (MeanT) and Euler number (Euler no.). Hydraulic properties include saturated hydraulic conductivity (K_{sat}) and unsaturated hydraulic conductivity (K_{unsat}).

Table 4 *Pearson correlation matrix for the CT derived macropore characteristics and log of measured hydraulic properties of soil. (Significant correlation at p value less than 0.01***, 0.05** and 0.1* is indicated)*

Variables	*Log K_{sat}*	*Log K_{unsat}*	*MP*	*MPC*	*D_{crit}*	*Aniso*	*FracD*	*MeanT*	*Euler no.*
Log K_{sat}	1.000								
Log K_{unsat}	0.613***	1.000							
MP	0.663***	0.824***	1.000						
MPC	0.662***	0.824***	0.989***	1.000					
D_{crit}	0.773***	0.358	0.470**	0.479**	1.000				
Aniso	-0.168	-0.355	-0.145	-0.150	-0.126	1.000			
FracD	0.409*	0.806***	0.813***	0.791***	0.239	-0.081	1.000		
MeanT	0.557**	-0.002	0.206	0.235	0.724***	-0.014	-0.175	1.000	
Euler no.	-0.422*	-0.117	-0.267	-0.283	-0.276	0.350	0.248	-0.455**	1.000

Selected correlations (significant at $p < 0.05$) were graphically displayed for X-ray CT derived macropore characteristics and saturated hydraulic conductivity. The log of saturated hydraulic conductivity [$\log_{10}(K_{sat})$] was plotted as function of X-ray CT derived macroporosity, connected macroporosity, critical pore diameter and mean thickness as shown in Fig 5. The strongest relationship was observed between critical pore diameter and saturated hydraulic conductivity with "r" of 0.77.

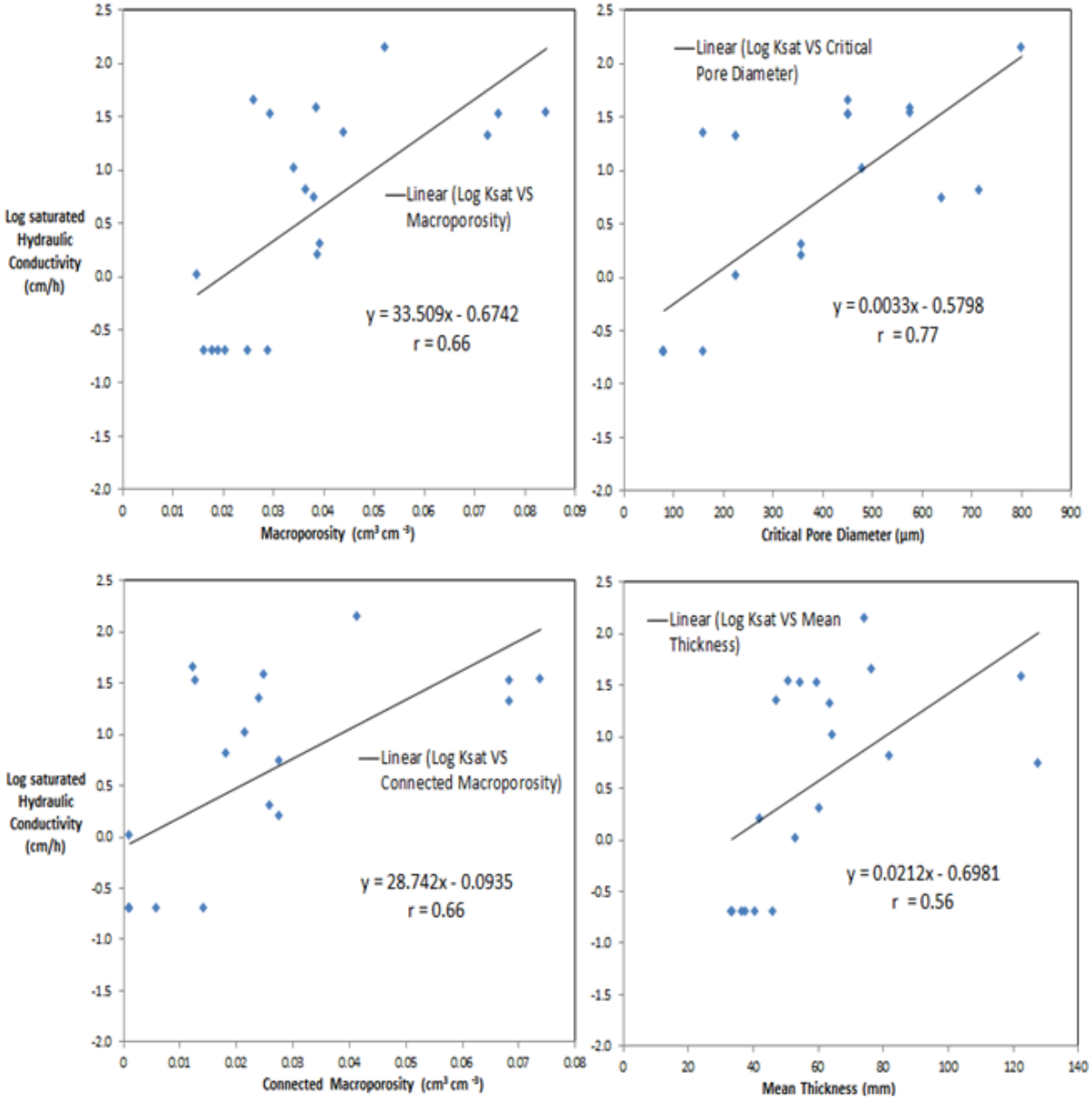

Figure 5 *Graphical representation of selected correlations (significant at $p < 0.05$) of [log_{10} (K_{sat})] against X-ray CT derived macroporosity, connected macroporosity, critical pore diameter and mean thickness.*

Selected correlations were graphically displayed for X-ray CT derived macropore characteristics and unsaturated hydraulic conductivity. The log of unsaturated hydraulic conductivity [$\log_{10}$ (K_{unsat})] was plotted as function of X-ray CT derived macroporosity, connected macroporosity, critical pore diameter and fractal dimension, as shown in Fig 6. The strongest relationships with log of unsaturated hydraulic conductivity [$\log_{10}$ (K_{unsat})] were observed for macroporosity (r = 0.82), connected macroporosity (r = 0.82) and fractal dimension (r = 0.80).

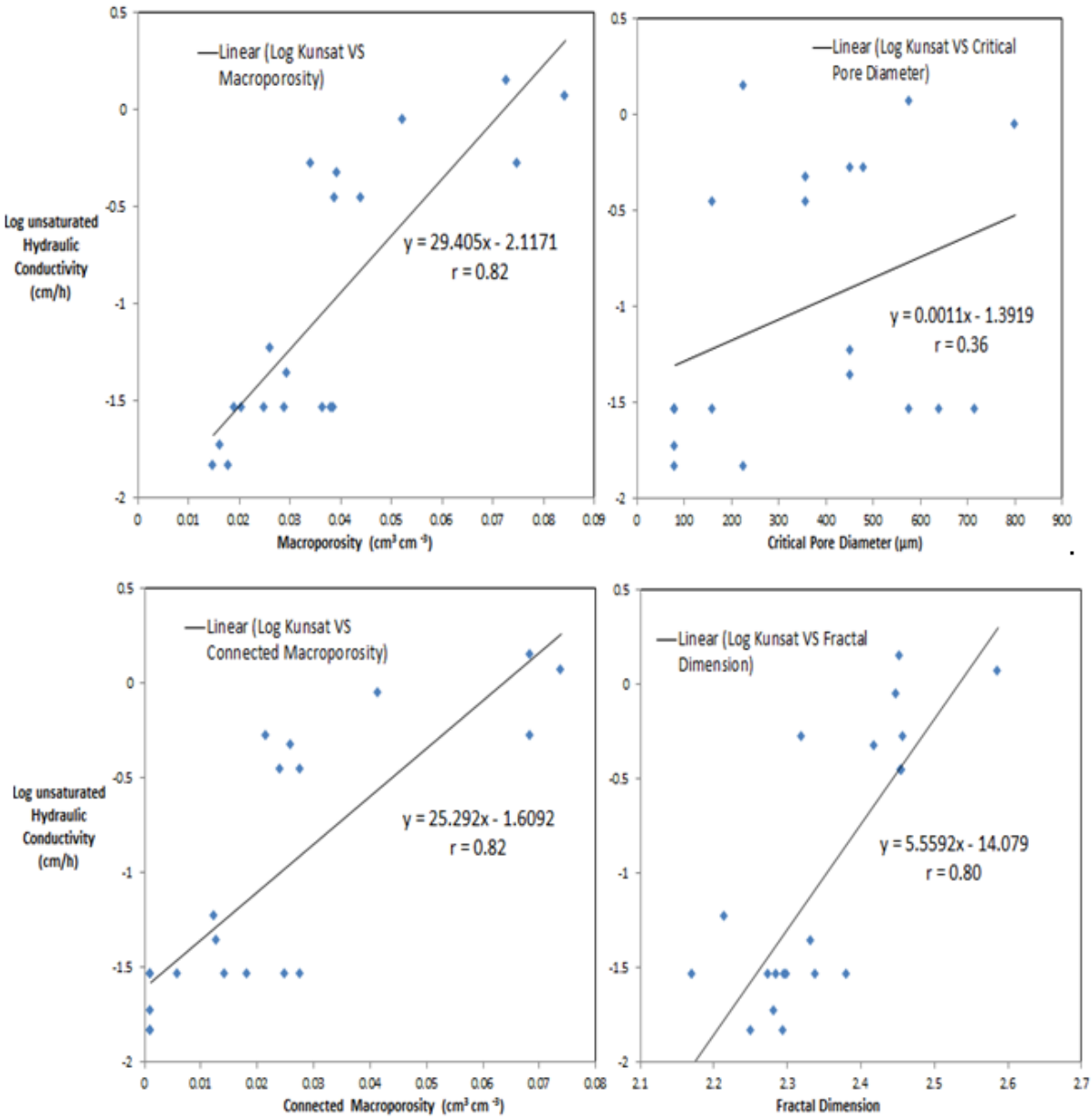

Figure 6 *Graphical representation of selected correlation of [log_{10} (K_{unsat})] against X-ray CT derived macroporosity, connected macroporosity, critical pore diameter and fractal dimension.*

Selected correlations (significant at $p < 0.05$) were graphically displayed for X-ray CT derived macropore characteristics showing interrelation (Fig 7). Strong linear regression between fractal dimension and macroporosity shows that the large macroporosities were associated with better macropore connectivity and larger macropore surface area. This space filling property of soil column with larger macroporosities is further indicated by the strong linear regression between macroporosity and connected macroporosity.

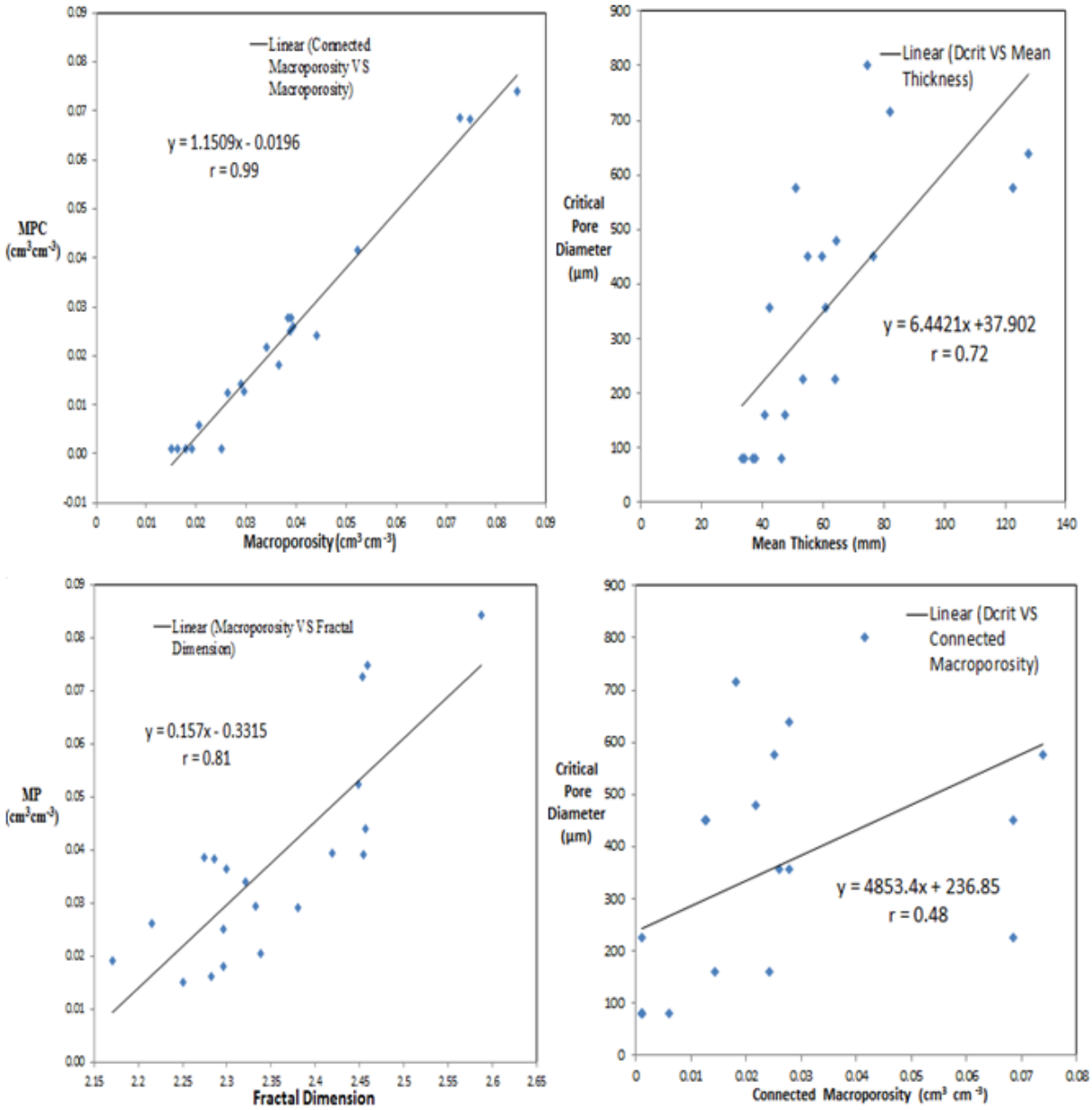

Figure 7 *Graphical representation of selected correlation (significant at $p < 0.05$) showing interrelation of macropore characteristics (connected macroporosity against macroporosity, critical pore diameter against mean thickness, and macroporosity against fractal dimension and critical pore diameter against connected macroporosity).*

4.4. Prediction of hydraulic properties based on macropore characteristics

The relationships between hydraulic conductivity and CT- derived macropore characteristics were developed using simple and multiple linear regression equations.

4.4.1. Saturated hydraulic conductivity

Table 5 shows the parameters of regression equation for predicting the log of saturated hydraulic conductivity from macropore characteristics. The p- value and r^2 suggest that critical pore diameter, macroporosity and connected macroporosity are the best parameters to predict the log of saturated hydraulic conductivity.

Table 5 *Parameter of regression equation for predicting the log of saturated hydraulic conductivity from the CT derived macropore characteristics*

Variables	Intercept	Slope	r^2	p-value	n
MP (cm^3cm^{-3})	-0.67	33.50914	0.44	0.00144	20
MPC (cm^3cm^{-3})	-0.09	28.74174	0.44	0.00149	20
D_{crit} (µm)	-0.58	0.00300	0.60	0.00006	20
Aniso	0.92	-1.43437	0.03	0.47888	20
FracD	-8.80	3.99214	0.17	0.07352	20
MeanT (mm)	-0.70	0.02125	0.31	0.01074	20
Eular no.	1.47	-0.00004	0.18	0.06382	20

Best subset linear regression was performed to calculate the best multiple linear regression equation for predicting the log of saturated hydraulic conductivity from the macropore characteristics as shown in Table 6.

Table 6 *Best multiple linear regression equation for predicting logarithm of the saturated hydraulic conductivity [log_{10} (K_{sat})] using CT derived macropore characteristics*

Dependent Variable	Best model equation	r^2	p-value	
			MPC	**D_{crit}**
Log of K_{sat} (cm/h)	16.409*(MPC) + 0.002*(D_{crit}) - 0.695	0.71	0.0215	0.0009
			MP	**D_{crit}**
Log of K_{sat} (cm/h)	19.404*(MP) + 0.002*(D_{crit}) - 1.037	0.71	0.0184	0.0008

It was observed that among many macropore characteristics, critical pore diameter gave the best results. The addition of macroporosity and connected macroporosity in a multiple linear regression with critical pore diameter improved the model performance as shown in Table 6. Macroporosity and connected macroporosity are not significant (at $p < 0.01$) so we may say that it is only the critical pore diameter that largely explains variation in the saturated hydraulic conductivity. Luo *et al.*, (2010) found that path number (the number of paths connected from top to bottom in a soil sample in the vertical direction) and macroporosity were the best predictor macropore parameters for saturated hydraulic conductivity. The fact that the critical pore diameter was the best macropore characteristic for predicting saturated hydraulic conductivity suggests that models based on percolation theory may give reliable predictions of Ksat. Percolation theory states that the bottleneck pores along the fastest connected flow path offers most of the resistance to flow. Thus these bottleneck pores can be considered to characterize the flow through the porous medium (Ewing & Hunt, 2009).

4.4.2. Unsaturated hydraulic conductivity

Table 7 shows the parameters of regression equation for predicting the log of unsaturated hydraulic conductivity from the macropore characteristics. The p- value and r^2 suggest that macroporosity, connected macroporosity and fractal dimension are the best parameters to predict the log of unsaturated hydraulic conductivity.

Table 7 *Parameter of regression equation for predicting the log of unsaturated hydraulic conductivity from the CT derived macropore characteristics*

Variables	Intercept	Slope	r^2	p-value	n
MP (cm^3cm^{-3})	-2.11712	29.40487	0.678709	0.00001	20
MPC (cm^3cm^{-3})	-1.60921	25.29183	0.679718	0.00001	20
D_{crit} (µm)	-1.39188	0.001084	0.128223	0.12109	20
Aniso	-0.50792	-2.13807	0.125797	0.12493	20
FracD	-14.0795	5.559199	0.649831	0.00002	20
MeanT (mm)	-1.00705	-5.6E-05	0.000004	0.99308	20
Eular no.	-0.83712	-8.3E-06	0.013707	0.62302	20

Best subset linear regression was performed to find the best multiple linear regression equation for predicting the log of unsaturated hydraulic conductivity from the macropore characteristics as shown in Table 8.

Table 8 *Best multiple linear regression equation for predicting logarithm of the unsaturated hydraulic conductivity [log_{10} (K_{unsat})] using CT derived macropore characteristics*

Dependent Variable	Best model equation	r^2	p-value	
			MP	**FracD**
Log of K_{unsat} (cm/h)	17.73*(MP) + 2.77*(FracD) - 8.19	0.73	0.033	0.078
			MPC	**FracD**
Log of K_{unsat} (cm/h)	15.31*(MPC) + 2.83*(FracD) - 8.04	0.74	0.023	0.056

It was observed that none of the macropore characteristics combinations that excluded macroporosity and connected macroporosity gave better results than macroporosity and connected macroporosity. The addition of fractal dimension with macroporosity and connected macroporosity increased the prediction from ($r^2 = 68$) to ($r^2 = 74$) in case of connected macroporosity and ($r^2 = 68$) to ($r^2 = 73$) for macroporosity. Fractal dimension is not significant (at $p < 0.05$), so we may conclude that only the macroporosity and connected macroporosity contributes significantly to unsaturated hydraulic conductivity.

5. Limitations

5.1. Saturated hydraulic conductivity

The connected macroporosity for column 17 (depth 70-75cm) was zero, but it had a saturated hydraulic conductivity of 0.2 cm/hour. This can be explained by the fact that connected pores smaller than our image resolution of 80 microns will have contributed to the saturated hydraulic conductivity. In contrast, some CT imaged pores were connected from top to bottom in column 19 (depth 70-75cm), but we did not record any saturated hydraulic conductivity. This can be explained by air entrapment in larger pores which obstructs the flow of water.

5.2. Unsaturated hydraulic conductivity

According to the capillary rise equation in case of unsaturated hydraulic conductivity, supplying water to the soil at -6 cm matric potential will exclude water flow through pores larger than 0.5 mm diameter during infiltration. But our images include larger pores that would not have contributed to the flow. The algorithm "pore thickness images" can be used to delete pores larger than 0.5 mm diameter using ImageJ. This should be done in future studies. It would also be interesting to identify changes in pore space characteristics after measuring hydraulic conductivity.

6. Conclusions

Strong correlations were found between near-saturated and saturated hydraulic conductivity of soil and X-ray CT derived macropore network characteristics. Among the macropore characteristics analyzed, saturated hydraulic conductivity is mainly controlled by the critical pore diameter (D_{crit}). Unsaturated hydraulic conductivity at -6 cm matric potential is mainly predicted by macroporosity and connected macroporosity. This result suggests that percolation-based models may be useful for predicting saturated hydraulic conductivity.

For predicting hydraulic properties of soil, the statistical approaches have a limited use for modelling purpose because of strong correlation between macropore characteristics. Therefore physics-based approaches like percolation models based on critical pore diameter provides best alternatives. We need more data to better identify which parameters are most important. In the future standard laboratory soil characterization can be complemented by X-ray CT derived data. X-ray CT derived macropore characteristics can be used for predicting the hydraulic properties of soil. This can lead towards digital soil physics laboratories in future.

Acknowledgements

Firstly I would like to thank my supervisors, Nicolas Jarvis and Johannes Koestel for their guidance and support throughout the research project. Thank you so much I have learned a lot during my research work with your group.

I would like to thank Ingmar Messing for being examiner and providing the valuable suggestions and comments during my presentation and on my thesis report. It turned out really well and improved my understanding about the topic.

I am really grateful to my opponent Maryia Babko for her valuable discussion and being taking the role of opponent for my thesis.

I also want to thank Mats Larsbo for supervising me in summer internship. That experience really improves my understanding about X-ray computed tomography.

References

Abràmoff, M. D., Magalhães, P. J. & Ram, S. J. (2004). Image processing with ImageJ. *Biophotonics international*, 11(7), pp 36–42.

Arrington, K. E., Ventura, S. J. & Norman, J. M. (2013). Predicting Saturated Hydraulic Conductivity for Estimating Maximum Soil Infiltration Rates. *Soil Science Society of America Journal*, 77(3), p 748.

Black, C. A., Miller, R. H., Page, A. L., Klute, A. & American Society of Agronomy (Eds) (2006). *Physical and mineralogical methods*. 2. ed., reprint. Madison, Wis: American Society of Agronomy. (Methods of soil analysis; spons. jointly by the American Society of Agronomy and American Society for Testing and Materials. Ed. C. A. Black ... ; Pt. 1). ISBN 978-0-89118-811-7.

Bouma, J. (1989). Using Soil Survey Data for Quantitative Land Evaluation. In: Stewart, B. A. (Ed) *Advances in Soil Science*. pp 177–213. Springer US. (9). ISBN 978-1-4612-8144-3.

Doube, M., Kłosowski, M. M., Arganda-Carreras, I., Cordelières, F. P., Dougherty, R. P., Jackson, J. S., Schmid, B., Hutchinson, J. R. & Shefelbine, S. J. (2010). BoneJ: Free and extensible bone image analysis in ImageJ. *Bone*, 47(6), pp 1076–1079.

Ewing, R. & Hunt, A. (2009). *Percolation Theory for Flow in Porous Media* [online]. Berlin, Heidelberg: Springer Berlin Heidelberg. Available from: http://link.springer.com/10.1007/978-3-540-89790-3. [Accessed 2016-05-25].

Feldkamp, L. A., Davis, L. C. & Kress, J. W. (1984). Practical cone-beam algorithm. *JOSA A*, 1(6), pp 612–619.

Iversen, B. V., Lamandé, M., Torp, S. B., Greve, M. H., Heckrath, G., de Jonge, L. W., Moldrup, P. & Jacobsen, O. H. (2012). Macropores and Macropore Transport: Relating Basic Soil Properties to Macropore Density and Soil Hydraulic Properties. *Soil Science*, 177(9), pp 535–542.

Jabro, J. D. (1992). Estimation of saturated hydraulic conductivity of soils from particle size distribution and bulk density data. *Transactions of the ASAE*, 35(2), pp 557–560.

Jarvis, N. J. (2007). A review of non-equilibrium water flow and solute transport in soil macropores: principles, controlling factors and consequences for water quality. *European Journal of Soil Science*, 58(3), pp 523–546.

Jarvis, N., Koestel, J., Messing, I., Moeys, J. & Lindahl, A. (2013). Influence of soil, land use and climatic factors on the hydraulic conductivity of soil. *Hydrology and Earth System Sciences*, 17(12), pp 5185–5195.

John Koestel (2016). SoilJ- An ImageJ plugin for semi-automatized image-processing of 3-D X-ray images of soil column. 18, p 4398.

Klute, A., Amoozegar, A. & Warrick, A. W. (1986a). Hydraulic Conductivity of Saturated Soils: Field Methods. *SSSA Book Series*. Soil Science Society of America, American Society of Agronomy. ISBN 978-0-89118-864-3.

Klute, A., Klute, A. & Dirksen, C. (1986b). Hydraulic Conductivity and Diffusivity: Laboratory Methods. *SSSA Book Series*. Soil Science Society of America, American Society of Agronomy. ISBN 978-0-89118-864-3.

Kværnø, S. H., Haugen, L. E. & Børresen, T. (2007). Variability in topsoil texture and carbon content within soil map units and its implications in predicting soil water content for optimum workability. *Soil and Tillage Research*, 95(1–2), pp 332–347.

Larsbo, M., Koestel, J. & Jarvis, N. (2014). Relations between macropore network characteristics and the degree of preferential solute transport. *Hydrology and Earth System Sciences*, 18(12), pp 5255–5269.

Lin, H. S., Mclnnes, K. J., Wilding, L. P. & Hallmark, C. T. (1999). Effect of Soil Morphology on Hydraulic Properties: II. Hydraulic Pedotransfer Functions. Soil Science Society of America Journal, 63, pp 955-961.

Luo, L., Lin, H. & Schmidt, J. (2010). Quantitative Relationships between Soil Macropore Characteristics and Preferential Flow and Transport. *Soil Science Society of America Journal*, 74(6), p 1929.

Messing, I. (1989). Estimation of the Saturated Hydraulic Conductivity in Clay Soils from Soil Moisture Retention Data. Soil Science Society of America Journal, 53, pp 665-668

Minasny, B. & McBratney, A. B. (2000). Evaluation and development of hydraulic conductivity pedotransfer functions for Australian soil. *Soil Research*, 38(4), pp 905–926.

Naveed, M., Moldrup, P., Arthur, E., Wildenschild, D., Eden, M., Lamandé, M., Vogel, H.-J. & de Jonge, L. W. (2013). Revealing Soil Structure and Functional Macroporosity

along a Clay Gradient Using X-ray Computed Tomography. *Soil Science Society of America Journal*, 77(2), p 403.

Nemes, A., Rawls, W. J. & Pachepsky, Y. A. (2005). Influence of Organic Matter on the Estimation of Saturated Hydraulic Conductivity. *Soil Science Society of America Journal*, 69(4), p 1330.

Paradelo, M., Katuwal, S., Moldrup, P., Norgaard, T., Herath, L. & de Jonge, L. W. (2016). X-ray CT-Derived Soil Characteristics Explain Varying Air, Water, and Solute Transport Properties across a Loamy Field. *Vadose Zone Journal*, 15(4), p 0.

Pierret, A., Capowiez, Y., Belzunces, L. & Moran, C. J. (2002). 3D reconstruction and quantification of macropores using X-ray computed tomography and image analysis. *Geoderma*, 106(3), pp 247–271.

Prewitt, J. & Mendelsohn, M. L. (1966). The analysis of cell images*. *Annals of the New York Academy of Sciences*, 128(3), pp 1035–1053.

Rawls, W. J., Gimenez, D. & Grossman, R. (1998). Use of soil texture, bulk density, and slope of the water retention curve to predict saturated hydraulic conductivity. *Transactions of the ASAE*, 41(4), p 983.

Soil Properties Laboratory - Ksat Lab procedures.pdf. Available from: http://munster.tamu.edu/BAEN672/Homework/Ksat%20Lab%20procedures.pdf. [Accessed 2016-06-09]

Smettem, K. R. J., Carlisle, P., Poulter, R. & Cook, S. E. (1999). Use of soil survey pedotransfer functions in spatial modelling of potential and actual wheat yields in precision agriculture., 1999. pp 539–549. Sheffield Academic Press.

Starkloff, T. & Stolte, J. (2014). Applied comparison of the erosion risk models EROSION 3D and LISEM for a small catchment in Norway. *CATENA*, 118, pp 154–167.

Vereecken, H., Weynants, M., Javaux, M., Pachepsky, Y., Schaap, M. G. & Genuchten, M. T. van (2010). Using Pedotransfer Functions to Estimate the van Genuchten–Mualem Soil Hydraulic Properties: A Review. *Vadose Zone Journal*, 9(4), p 795.

Viggiani, G., Ando, E., Takano, D., & Santamarina, J. C. (2015). Laboratory X-ray Tomography: A Valuable Experiment Tool for Revealing Processess in Soils. Geotechnical Testing Journal, 38(1), pp 61-71.

Wagner, B., Tarnawski, V. R., Wessolek, G. & Plagge, R. (1998). Suitability of models for the estimation of soil hydraulic parameters. *Geoderma*, 86(3–4), pp 229–239.